ADVANCED ENERGY MATERIALS
www.advenergymat.de

In Situ TEM Observation of Electrochemical Lithiation of Sulfur Confined within Inner Cylindrical Pores of Carbon Nanotubes

*Hyea Kim, Jung Tae Lee, Alexandre Magasinski, Kejie Zhao, Yang Liu, and Gleb Yushin**

Lithium insertion into sulfur confined within 200 nm cylindrical inner pores of individual carbon nanotubes (CNTs) was monitored in situ in a transmission electron microscope (TEM). This electrochemical reaction was initiated at one end of the S-filled CNTs. The material expansion during lithiation was accommodated by the expansion into the remaining empty pore volume and no fracture of the CNT walls was detected. A sharp interface between the initial and lithiated S was observed. The reaction front was flat, oriented perpendicular to the confined S cylinder, and propagated along the cylinder length. Lithiation of S in the proximity of conductive carbon proceeded at the same rate as the one in the center of the pore, suggesting the presence of electron pathways at the Li_2S/S interface. Density of states calculations further confirmed this hypothesis. In situ electron diffraction showed a direct phase transformation of S into nanocrystalline Li_2S without detectable formation of any intermediates, such as polysulfides and LiS. These important insights may elucidate some of the reaction mechanisms and guide the improvements in the design of C–S nanocomposites for high specific energy Li–S batteries. The proposed use of conductive CNTs with tunable pore diameter as cylindrical reaction vessels for in situ TEM studies of electrochemical reactions proved to be highly advantageous and may help to resolve the ongoing problems in battery technology.

1. Introduction

The development of high specific energy rechargeable lithium and lithium ion batteries (LIBs) now attracts world's attention because the life of the majority of population is inextricably linked to batteries. The capacity of batteries has a great impact on many aspects of our life and the capacity limitations become particularly hurtful at the age of the rapidly developing portable electronic devices and electrical vehicles (EVs). As the technology of the current state-of-the-art LIBs based on Li intercalation compounds is approaching its limits, many scientists are exploring alternative battery materials' chemistries.[1]

Among many candidates, sulfur (S) and S-based materials are considered to be the most promising cathodes[2,3] since S provides extremely high theoretical specific capacity (1672 mAh g^{-1}), nearly an order of magnitude higher than that of the traditional lithium cobalt oxide (LCO).[4] S is also an inexpensive, nontoxic, easy to handle, safe, and environmentally benign material. Intense research over the past decade has resulted in the significant improvements in cycle life (>1000 cycles now demonstrated in selected cells) and accessible capacity (now approaching its theoretical value). However, multiple shortcomings in S–Li chemistry still exist and need to be overcome to achieve technology commercialization.[5] These include the low intrinsic electronic conductivity of S, high volume changes, dissolution of intermediate reaction products, to name a few. For example, low conductivity of S is believed to require significant portion of the active material mass to be replaced by conductive additives, such as carbon. The relatively high volume expansion (≈80%) of S during lithiation can induce electrode damage and cell degradation. Another significant problem is associated with the dissolution of the intermediate products, high-order lithium polysulfides (Li_2S_n, $4 \le n \le 8$), into the organic electrolytes, resulting in an active mass loss and growing cell resistance due to the increase in electrolyte viscosity and redeposition of the sulfide layer on the surface of both electrodes, which blocks electrolyte pathways.[6] Such problem is particularly severe for thicker electrodes.

Attempts to overcome existing challenges with S-based cathodes often involve encapsulating or trapping the S/Li_2S active material as well as polysulfides intermediate within the conductive host materials,[7,8] such as carbon. However, the detailed mechanisms and pathways of electrochemical reactions of Li with S at the nanoscale remain unclear. Real-time observations conducted during such reaction(s) would provide the most powerful insights needed to fill the existing gap in

Dr. H. Kim, J. T. Lee, Dr. A. Magasinski, Prof. G. Yushin
School of Materials Science and Engineering
Georgia Institute of Technology
Atlanta, GA 30332, USA
E-mail: yushin@gatech.edu
Dr. H. Kim
Sila Nanotechnologies, Inc.
Alameda, CA 94502, USA
Prof. K. Zhao
School of Mechanical Engineering
Purdue University
West Lafayette, IN 47906, USA
Dr. Y. Liu
Center for Integrated Nanotechnologies
Sandia National Laboratory
Albuquerque, NM 87185, USA

DOI: 10.1002/aenm.201501306

knowledge and provide the highly needed guidelines for the effective design of reliable S electrodes and Li–S cells. Previous report[9] using synchrotron-based in operando X-ray diffraction (XRD) showed formation of amorphous Li_2S during discharge, which was contrary to the most previously published ex situ experimental results and our own observations.[9,10] However, the authors did observe formation of crystalline Li_2S when the discharged cell is allowed to rest.[9] Synchrotron studies, however, does not provide information about the local interactions at the nanoscale and report averaged data instead.

In this study, we report on the first real-time observation of lithiation of S confined within a cylindrical carbon pore in situ using a specialized holder within a transmission electron microscope (TEM). This in situ TEM electrochemistry technique is a powerful tool to understand the dynamic processes of electrochemical reactions of battery materials at a high spatial resolution from which the morphological evolution, phase transformation, and chemical composition changes can be revealed.[11] Template-synthesized multiwalled carbon nanotube (CNT)[12,13] was used as a reaction vessel in order to prevent S evaporation during heating, provide structural support and, supply electrons to electrochemical reaction sites. The advantages of this approach include the ability to precisely control diameter of the conductive vessel and the possibility to confine electrochemically active material (such as S) strictly inside the inner pore of the tube (preventing S deposition on the outer CNT surface). Formation of new phases during electrochemical reaction was studied simultaneously (in situ) by using electron diffraction technique.

2. Results and Discussion

One of the critical issues in conducting in situ TEM observations of the electrochemical reaction of sulfur (and other insulating materials with low melting point) is a preparation of a suitable reaction vessel. We demonstrate that CNTs serve well for this purpose—they have sufficiently small interstitials to prevent S diffusion through the pore walls and mitigate evaporation during heating by electron gun and sublimation in the high-vacuum environment inside the TEM. High thermal conductivity of CNTs[14] may also help to remove some of the adsorbed heat. Equally important, CNTs are sufficiently strong to support S expansion during lithiation without crack formation and mechanical failure. Their 1D structure helps to observe propagation of the electrochemical reaction front.

Figure 1 shows steps involved in the sample preparation. First, anodic aluminum oxide membranes with a pore size of ≈200 nm (Figure 1a) were placed in a quartz tube, heated in nitrogen (N) atmosphere to 700 °C and coated with ≈15 nm layer of carbon via C_3H_6 decomposition at atmospheric pressure (Figure 1b).[12] After cooling to room temperature, the carbon-coated alumina was then dipped into a molten S at 160 °C, where S filled the open sample pores (Figure 1c). The excess of S covering the top and the bottom surface of the membrane was removed by heating the sample at 250 °C in open air for 10 min (Figure 1d). Then the alumina template was etched with 10% hydrofluoric acid (HF) overnight. The HF was rinsed out with DI water at least 10 times and the pH was checked for a completion of rinsing process. Then the S/CNT bundles were dispersed in ethanol using an ultrasonicator (Figure 1e).

Figure 2a shows the TEM image of a typical S-in-CNT reaction vessel sample. A single CNT with ≈15 nm wall thickness and ≈200 nm cylindrical pore was observed. The hollow center is partially filled with S, as confirmed by energy dispersive X-ray spectroscopy (EDS) line scan (Figure 2b). No Al residues could be detected.

A miniaturized electrochemical cell consisting of S-in-CNT samples as a working electrode (WE) and Li as a counter/reference electrode (CE/RE) was used in a specialized nanofactory TEM scanning tunneling microscopy (STM) sample holder with

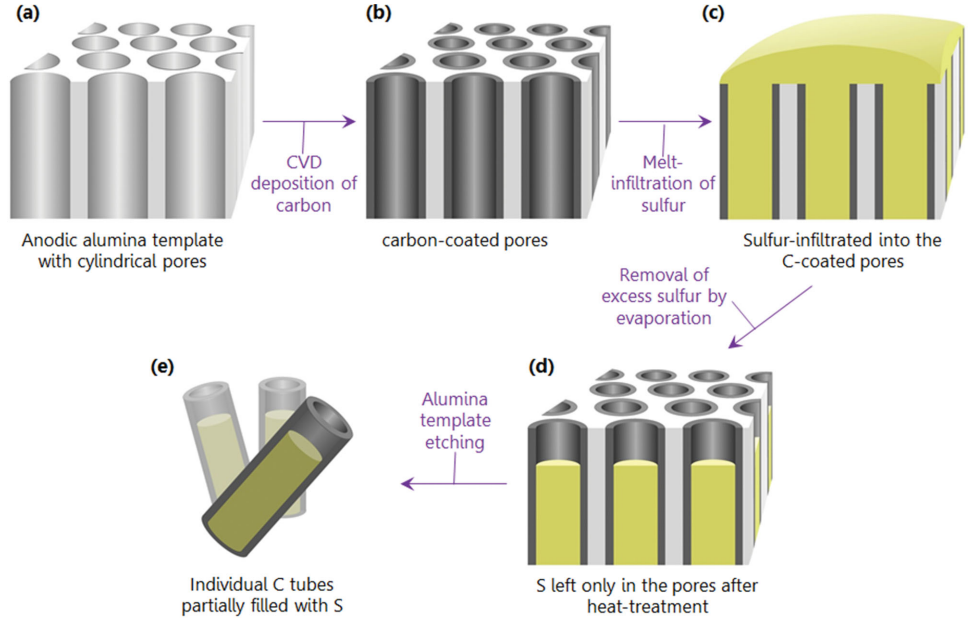

Figure 1. Schematic illustration of the individual S-in-CNT reaction vessel sample preparation process.

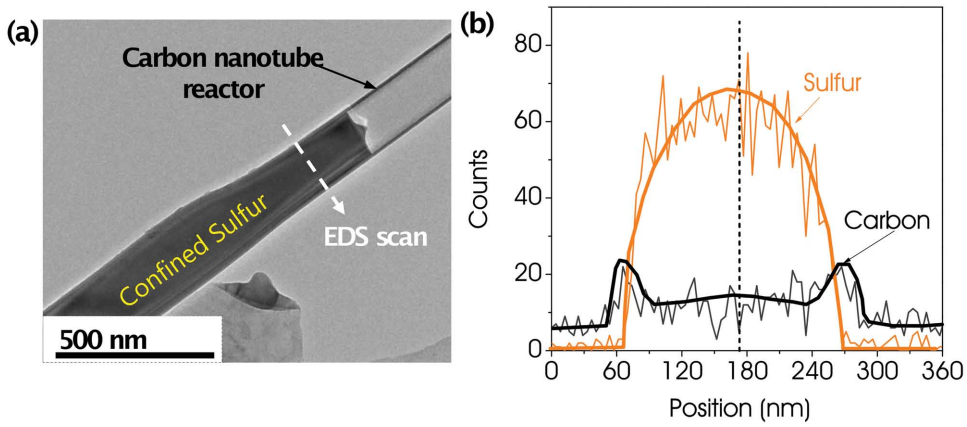

Figure 2. A typical S-in-CNT reaction vessel sample for in situ studies: a) TEM image and b) its corresponding cross-section EDS line scan.

3D piezo control and an external potentiostatic controller,[15] more detailed preparation is described in the Supporting Information. The Li was scratched from a fresh cut bulk Li metal surface inside a glove box and then it was exposed to air for about 2 s in the transfer of the holder into TEM, during which a naturally oxidized Li_2O layer was grown on the surface that can be served as an Li ion conducting solid electrolyte. **Figure 3** provides a schematic of this experimental setup. Using a piezo manipulator, the Li_2O/Li electrode was driven to contact with one of the selected S-in-CNT samples. Lithiation reaction was controlled by applying a constant potential hold to the WE versus CE/RE. Potentials of −2 V versus Li/Li^+ were typically applied to drive the lithiation reaction.

Due to a relatively low evaporation point of S, its TEM studies are known to be challenging. The advantages of using CNT nanoreactors include their help in dissipating heat and retaining the S under electron beam and vacuum within TEM. By conducting initial experiments under no applied bias we could evaluate stability of our S-in-CNT samples under different magnifications and electron beam brightness regimes and select suitable operating conditions, which correspond to the minimal losses of S within the time frame of our experiments. **Figure 4** shows three selected TEM images captured during the lithiation process into the S-in-CNT samples and their corresponding electron diffraction patterns (EDP) (the video recording part of the process can be found in the Supporting Information (movie S1)). The bottom-left corner of the CNT sample is in a direct contact with LiO_2-coated Li. Initially, only a uniform crystalline phase of S exists inside a portion of the hollow CNT reaction vessel (dark region in Figure 4a). The EDP confirmed the S_8 crystalline structure of the sulfur filler (Figure 4d). As the lithiation process proceeds, a clear contrast change of the filler from a dark to a light phase (Figure 4b) is observed. The electron diffraction studies revealed that light region corresponds to a polycrystalline Li_2S phase (Figure 4e,f). From the abrupt contrast change, the movement of the reaction front could be monitored till all S were transformed to Li_2S.

In our previous studies we have successfully conducted high-resolution TEM studies on 5–20 nm Li_2S nanoparticles embedded into a carbon matrix.[16] In this case, high thermal conductivity of carbon dissipated heat very efficiently, minimizing the focused beam-induced sample damage. Unfortunately, we could not conduct similar studies on 200 nm diameter samples. Because a very high intensity of the beam is concentrated in a very small area of thermally isolative and relatively large S/Li_2S, the electron beam was inducing significant damages to the sample (see Figure S1, Supporting Information).

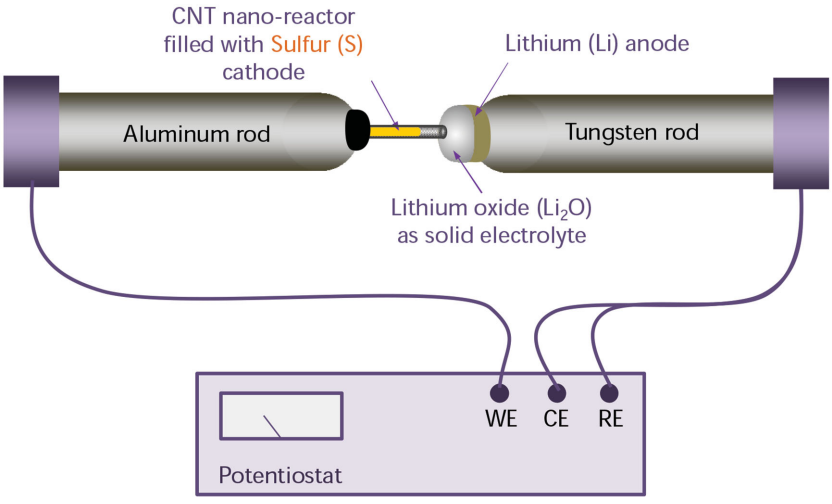

Figure 3. Schematic illustration of the electrochemical device set up for a real-time TEM observation of an electrochemical lithiation of nanoconfined S cathodes.

Figure 5 shows higher resolution of the Li_2S phase region (Figure 5a) and the corresponding EDP pattern, revealing 5–50 nm size of the Li_2S grains. No other phases could be detected by EDP (Figure 5b). To further confirm the lithiation of sulfur inside CNTs, electron energy loss spectroscopy (EELS) was carried out on individual S-in-CNT sample before and after lithiation. The EELS spectra from pristine (black curve) and fully lithiated S-in-CNT (red curve) are presented in **Figure 6**. The rise of Li–K edge peaked around 58 eV indicates the lithium insertion into the

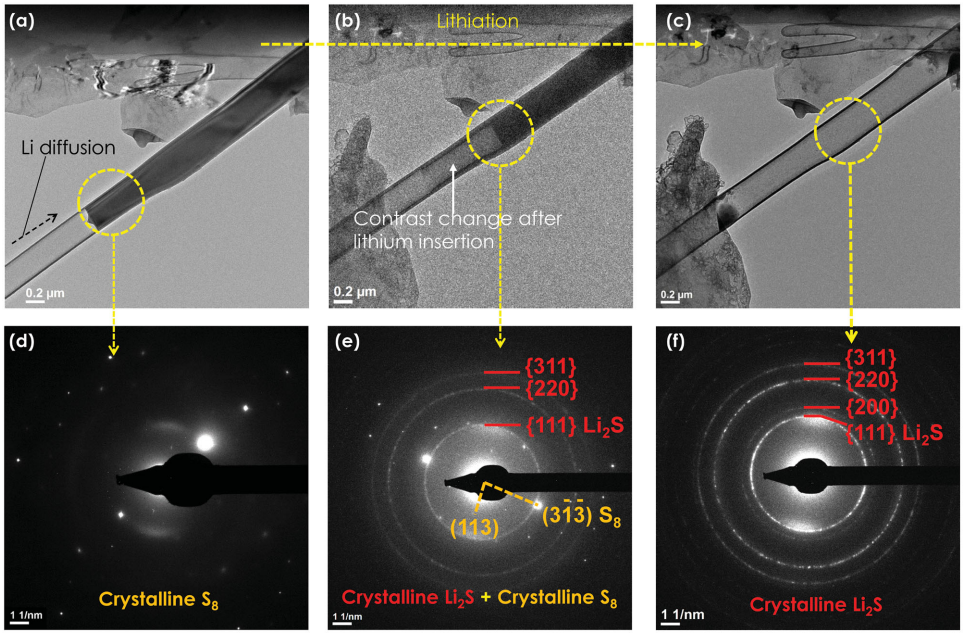

Figure 4. Selected images of the sample evolution during a typical lithiation process: a–c) TEM images captured during lithiation of S nanoconfined in a CNT reaction vessel and d–f) their corresponding EDP patterns; panels (a) and (d) correspond to the sample before the initiation and panels (c) and (f) after the completion of the electrochemical reaction. The darker area appearing at the bottom left corner of the CNT in panel (c) is a contaminant.

S-in-CNT sample after lithiation, as shown in Figure 6a. A ≈6 eV chemical shift in the S–L edge (with an onset energy about 159 eV) upon lithiation was observed (Figure 6b). The change of the shape of the S–L edge may indicate the transition from pure S_8 to polycrystalline Li_2S. We also note that the C–K edge peak changes shape, which may be related to both Li insertion and also overlap with the broad tail of S–L edge.

Several intriguing observations could be made from our studies. First, the reaction front is very flat and propagates along the axis of CNT (i.e., axial lithiation) in contrast to our initial expectations that core–shell lithiation behavior would be observed.[17] Specifically, we expected that S located close to C will react first with lithium producing Li_2S because both S and Li_2S have very low electronic conductivity[8,18] (with Li_2S being even less electronically conductive) and because any electrochemical reaction requires supply of electrons. We further expected that the lithiation would progress from the CNT/S interface into the center of the tube (i.e., core–shell lithiation), which evidently was not the case.

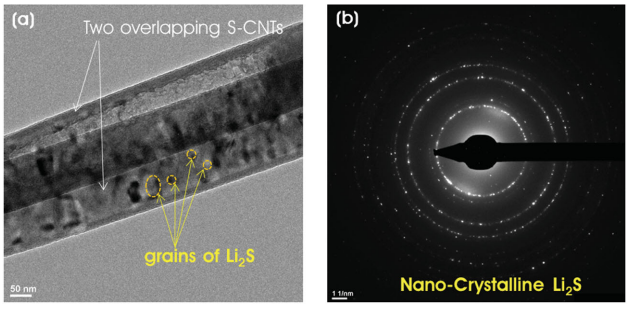

Figure 5. a) TEM image showing formation of 5–50 nm Li_2S grains in the lithiated area of the sample and b) the corresponding EDP.

Second, as we repeated the lithiation several times with fresh S-in-CNT samples the reaction rate was always constant with time (at ≈1 nm s^{-1}, calculated from several lithiation videos by measuring the times and the lengths of the corresponding lithiation paths), suggesting that the reaction rate was controlled by the interface (phase transformation) but not by the diffusion of the reaction species (Li ions and electrons) to the electrochemical reaction sites.

Third, in spite of the ≈80% volume expansion of S during lithiation, we did not observe a clear diameter change in CNT or fracturing of the CNT. We propose that due to a relatively week Van-der-Waals bonding between the CNT and both Li_2S, the extra volume needed is accommodated by squeezing out both fillers toward the ends of the CNT vessel. Mechanical strength of the produced CNTs was evidently high to withstand the induced stresses. In addition, we cannot exclude the possibility that volatility of S in high vacuum under constant electron bombardment (and thus heating to elevated temperatures) may lead to some of the S losses.

Fourth, we did not observe any bulk intermediate phases (polysulfides or LiS) during the transformation reaction. Indeed, from the EDP results in Figure 4, it is clear that the rings assigned to electron diffraction on nanocrystalline Li_2S become stronger and the spots assigned to electron diffraction on single crystalline S_8 become weaker and eventually disappear as the lithiation proceeds (the final phase is pure Li_2S). This phase transformation was also recorded by in situ electron diffraction shown in Movie S2 in the Supporting Information. We see only crystalline S_8 and Li_2S phases at the interface in the middle of the lithiation process (Figure 4e) with no signs of the amorphous or polycrystalline intermediate products, such as Li_2S_2, Li_2S_4, etc., in contrast to our initial expectations based on the prior studies of regular cells, where electrochemical reaction

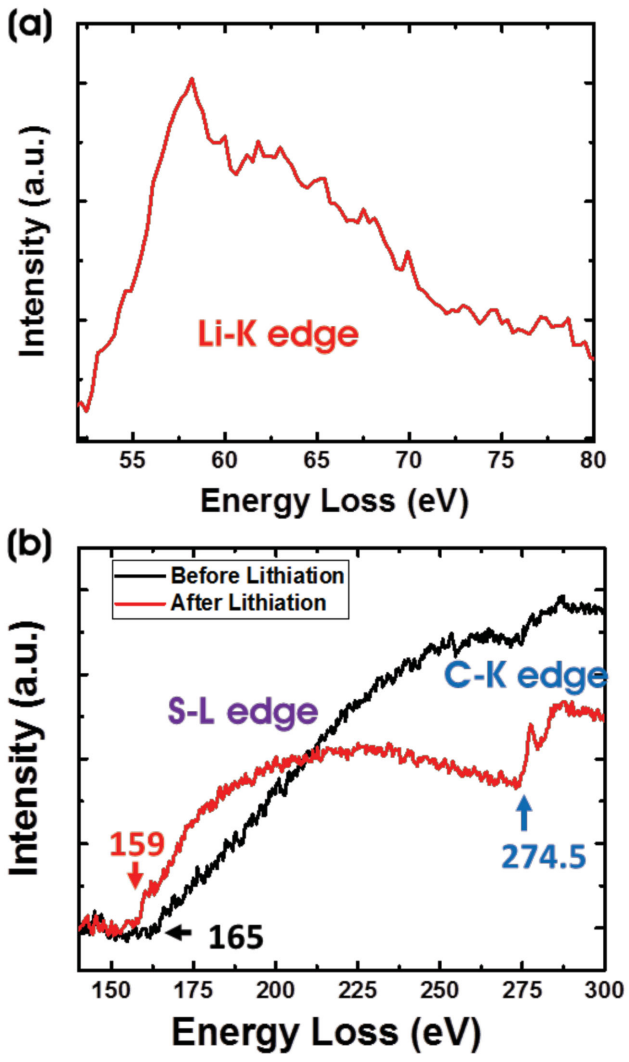

Figure 6. Electron energy loss spectra (EELS) of an individual S-in-CNT before (black curve) and after lithiation (red curve): a) Li–K edge, showing the insertion of Li into the sample, b) S–L and C–K edges, showing a ≈6 eV chemical shift of onsite energy of the S–L peak after the lithiation.

proceeds with liquid electrolytes. We shall also note that our final phase of Li_2S is crystalline (Figures 4 and 5), which is contrary to amorphous phase observed at the end of discharge.[9] It is worth noticing that the diffraction rings from CNT {0002} planes can be observed in all the EDPs, and the Li ions can intercalate into the distorted sidewalls.

Figure 7 shows the proposed model of the lithiation process, which explains our observations. The pathways for the transport of Li^+ from the source (left) include the bulk and the surface of the CNT walls. While the Li^+ ion diffusion is slow in pure S, it is higher in bulk Li_2S (conductivity ≈10^{-13} S cm^{-1}).[19] More importantly, the grain-boundary Li conductivity of polycrystalline Li_2S is very high, allowing fabrication of some of the most conductive solid electrolytes comprising nanostructured Li_2S.[20] Therefore, once Li^+ ions reach nanocrystalline Li_2S, we shall expect a large portion of the Li flux to transport through the Li_2S filler toward the reaction front. The transport of electrons from the right side of the reaction vessel proceeds along the conductive CNT walls. Since both Li_2S and S are electrically isolative, we propose that electrons diffuse to the reaction front via a very thin, yet sufficiently electrically conductive Li_2S/S interfacial layer. Based on the experimental results (Figure 4), the electron transport to the interface is so fast that it is not even a rate-limiting step for this electrochemical reaction. If the reaction would proceed near the CNT surface, it would quickly build an electrically isolative Li_2S and the reaction would stop when sufficiently thick electrically isolative layer is built.

In order to gain additional support for the proposed model (Figure 7), we have calculated the electron density of states (DOS) in sulfur, several predicted intermediate disordered polysulfide phases (Li_2S_8 and Li_4S_8), and lithium sulfides (LiS and Li_2S), as shown in **Figure 8**. The Fermi energies have been shifted to zero of the energy scale. The corresponding DOS of pure S has a clear insulator character with a band gap (E_g) of ≈2.5 eV. When the Li concentration increases, Li donates electrons and the E_g quickly decreases. A clear transition of insulator to conductor occurs with more electronic states introduced around the Fermi energy level. We see that the band gap in Li_2S_8 and LiS disappears completely and in Li_4S_8 it remains very small (Figure 8a), suggesting significant electrical conductivity of these phases even at room temperature. However, when the composition reaches Li_2S, the band gap opens up again and the material shows the insulator characteristics. The insulator–conductor–insulator transition shows the intriguing fact that the Li insertion dynamically alters the electronic property of the polysulfides. The intermediate states of the conductive nature serve as the electron carriers and enable the reaction front to proceed with sufficient electron supplies.

The selected Li–S compositions are representative to the phases that may exist in the very short range of our reaction interface. While our experimental observation did not detect formation of polysulfides and LiS in the bulk, the electronic structure of the Li_2S/S interface should be similar to that of polysulfides. Formation of the conductive Li_2S/S interface layer likely plays a critical role of electron carriers for the redox reactions and supports the proposed model (Figure 7). The presence of the electrically conductive interface (or the electrically conductive interphases) may explain why large S and Li_2S particles show unexpectedly high electrochemical activity in Li/S cells.[3]

The absence of clearly detected polysulfide phases (Figure 4e) suggests that a direct transformation from S to Li_2S may become energetically (or kinetically) favorable during S lithiation reactions, particularly in the absence of a liquid electrolyte. We would like to clarify that polysulfides are not thermodynamically stable; they do not exist in the Li–S binary phase diagram. Their presence in regular cells is likely associated with the use of liquid electrolyte(s). At the same time, single plateau previously observed in Li/S cells[21] (particularly in those where no virtually direct contact between S(Li_2S) and liquid electrolyte exist) may suggest that similar direct transformations may also proceed in regular cells and thus a highly undesirable polysulfide shuttle[22] could be avoided.

Finally, we would like to caution our readers that our findings should not be generalized. Changing electrochemical environment from regular cells (commonly with liquid electrolyte) to that of the solid-state reactions in vacuum may impact

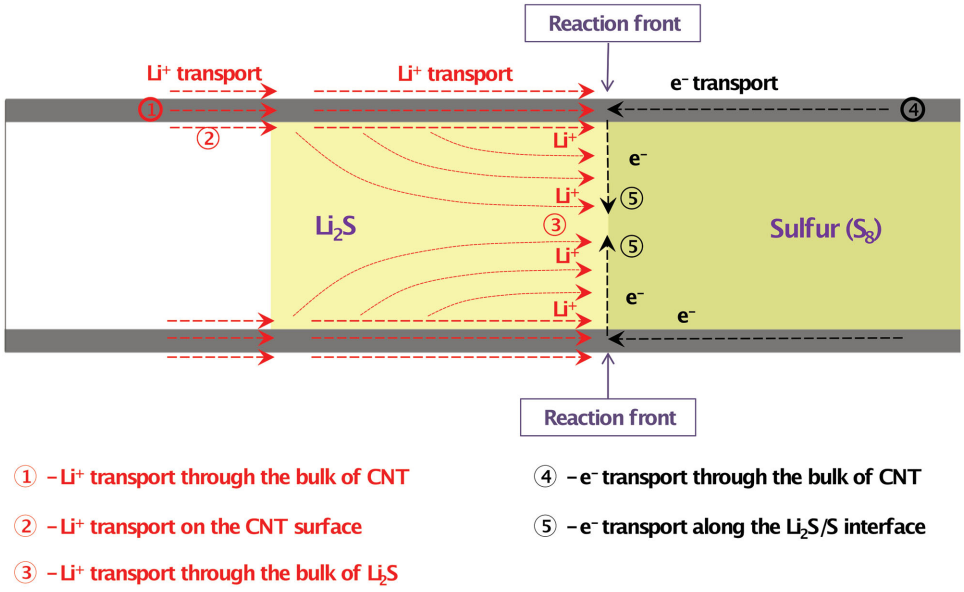

Figure 7. Proposed model of the electrochemical reaction of Li ions with S nanoconfined in a CNT, resulting in a flat, linearly propagating reaction front.

the reaction pathways. Electron beam may additionally change the phase transformation kinetics and lead to some evaporation of the active material. Yet, we believe that our findings provide valuable insights and guidance for further development of Li/S cell technologies.

3. Summary

In summary, electrochemical lithiation of sulfur nanoconfined in cylindrical pores was successfully visualized using in situ TEM studies for the first time. CNTs produced using CVD deposition of carbon onto an anodic alumina template proved to serve as excellent reaction vessels for such studies. Under a constant potential, the lithiation progressed linearly with time in the direction along the S-in-CNT orientation. The reaction front was flat, indicating that electrically isolative S not in a direct contact with conductive C can still be fully utilized. The observed lithiation behavior suggests that the Li_2S/S interfacial region is electrically conductive. Our numerical modeling results support this hypothesis. Such finding may explain the previously observed high-capacity utilization of cathodes comprising large electrically isolative particles of S or Li_2S. In situ electron diffraction studies demonstrate the possibility of a direct conversion of S into Li_2S without formation of polysulfide phases that exhibit high solubility in commonly used electrolytes. Our studies suggest the proposed in situ TEM technique with the active material encased within a nanosized

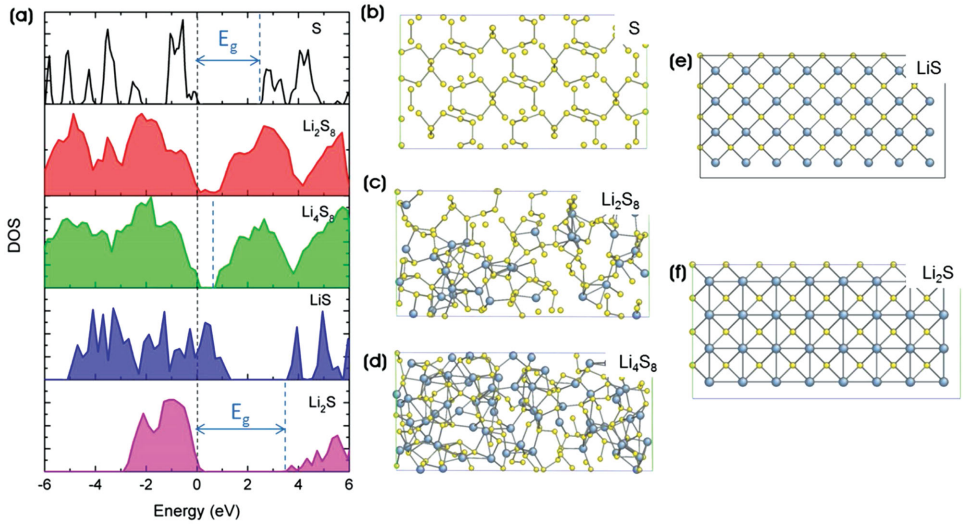

Figure 8. a) DOS of S, Li_2S_8, Li_4S_8, LiS and Li_2S and b–f) their corresponding crystal structures, demonstrating significant changes in the electronic structure of S during its lithiation, such as the disappearance of the band gap (E_g) in Li_2S_8 polysulfide.

electrically and ionically conductive electrochemical reactor to be a powerful tool for elucidating pathways for electrochemical reactions of conversion-type electrode materials.

Supporting Information

Supporting Information is available from the Wiley Online Library or from the author.

Acknowledgements

This work was partially supported by US ARO (grant W911NF-12-1-0259). This work was performed, in part, at the Center for Integrated Nanotechnologies, an Office of Science User Facility operated for the U.S. Department of Energy (DOE) Office of Science. Sandia National Laboratories is a multiprogram laboratory managed and operated by Sandia Corporation, a wholly owned subsidiary of Lockheed Martin Corporation, for the U.S. Department of Energy's National Nuclear Security Administration under contract DE-AC04-94AL85000.

Received: July 1, 2015
Revised: August 24, 2015
Published online: October 26, 2015

[1] a) B. Scrosati, J. Hassoun, Y.-K. Sun, *Energy Environ. Sci.* **2011**, *4*, 3287; b) N. Nitta, G. Yushin, *Part. Part. Syst. Charact.* **2014**, *31*, 317; c) B. Scrosati, J. Garche, *J. Power Sources* **2010**, *195*, 2419; d) J.-M. Tarascon, M. Armand, *Nature* **2001**, *414*, 359; e) M. S. Whittingham, *Chem. Rev.* **2004**, *104*, 4271; f) N. S. Choi, Z. Chen, S. A. Freunberger, X. Ji, Y. K. Sun, K. Amine, G. Yushin, L. F. Nazar, J. Cho, P. G. Bruce, *Angew. Chem., Int. Ed.* **2012**, *51*, 9994.

[2] a) H. Kim, F. Wu, J. T. Lee, N. Nitta, H. T. Lin, M. Oschatz, W. I. Cho, S. Kaskel, O. Borodin, G. Yushin, *Adv. Energy Mater.* **2015**, *5*, 1401792, 1401792; b) X.-B. Cheng, J.-Q. Huang, H.-J. Peng, J.-Q. Nie, X.-Y. Liu, Q. Zhang, F. Wei, *J. Power Sources* **2014**, *253*, 263; c) Z. Wei Seh, W. Li, J. J. Cha, G. Zheng, Y. Yang, M. T. McDowell, P.-C. Hsu, Y. Cui, *Nat. Commun.* **2013**, *4*, 1331; d) W. Li, G. Zheng, Y. Yang, Z. W. Seh, N. Liu, Y. Cui, *Proc. Natl. Acad. Sci. USA* **2013**, *110*, 7148; e) M.-K. Song, Y. Zhang, E. J. Cairns, *Nano Lett* **2013**, *13*, 5891.

[3] a) F. Wu, A. Magasinski, G. Yushin, *J. Mater. Chem. A* **2014**, *2*, 6064; b) F. Wu, J. T. Lee, A. Magasinski, H. Kim, G. Yushin, *Part. Part. Syst. Charact.* **2014**, *31*, 639.

[4] A. Manthiram, Y. Fu, S.-H. Chung, C. Zu, Y.-S. Su, *Chem. Rev.* **2014**, *114*, 11751.

[5] a) A. Manthiram, Y. Fu, Y.-S. Su, *Acc. Chem. Res.* **2012**, *46*, 1125; b) M.-K. Song, E. J. Cairns, Y. Zhang, *Nanoscale* **2013**, *5*, 2186; c) X. Ji, L. F. Nazar, *J. Mater. Chem.* **2010**, *20*, 9821; d) N. Nitta, F. Wu, J. T. Lee, G. Yushin, *Mater. Today* **2015**, *18*, 252.

[6] H. Yamin, A. Gorenshtein, J. Penciner, Y. Sternberg, E. Peled, *J. Electrochem. Soc.* **1988**, *135*, 1045.

[7] a) S. Evers, L. F. Nazar, *Acc. Chem. Res.* **2013**, *46*, 1135; b) H. Kim, J. T. Lee, G. Yushin, *J. Power Sources* **2013**, *226*, 256; c) R. Elazari, G. Salitra, A. Garsuch, A. Panchenko, D. Aurbach, *Adv. Mater.* **2011**, *23*, 5641; d) J. T. Lee, Y. Zhao, S. Thieme, H. Kim, M. Oschatz, L. Borchardt, A. Magasinski, W.-I. Cho, S. Kaskel, G. Yushin, *Adv. Mater.* **2013**, *25*, 4573; e) S. Moon, Y. H. Jung, W. K. Jung, D. S. Jung, J. W. Choi, D. K. Kim, *Adv. Mater.* **2013**, *25*, 6547; f) D. S. Jung, T. H. Hwang, J. H. Lee, H. Y. Koo, R. A. Shakoor, R. Kahraman, Y. N. Jo, M.-S. Park, J. W. Choi, *Nano Lett.* **2014**, *14*, 4418; g) J. Guo, Y. Xu, C. Wang, *Nano Lett.* **2011**, *11*, 4288.

[8] N. Jayaprakash, J. Shen, S. S. Moganty, A. Corona, L. A. Archer, *Angew. Chem.* **2011**, *123*, 6026.

[9] J. Nelson, S. Misra, Y. Yang, A. Jackson, Y. Liu, H. Wang, H. Dai, J. C. Andrews, Y. Cui, M. F. Toney, *J. Am. Chem. Soc.* **2012**, *134*, 6337.

[10] a) H. S. Ryu, Z. Guo, H. J. Ahn, G. B. Cho, H. Liu, *J. Power Sources* **2009**, *189*, 1179; b) S. Jeong, Y. Lim, Y. Choi, G. Cho, K. Kim, H. Ahn, K. Cho, *J. Power Sources* **2007**, *174*, 745; c) S.-E. Cheon, K.-S. Ko, J.-H. Cho, S.-W. Kim, E.-Y. Chin, H.-T. Kim, *J. Electrochem. Soc.* **2003**, *150*, A796.

[11] a) X. H. Liu, Y. Liu, A. Kushima, S. Zhang, T. Zhu, J. Li, J. Y. Huang, *Adv. Energy Mater.* **2012**, *2*, 722; b) C.-M. Wang, *J. Mater. Res.* **2015**, *30*, 326; c) M. Gu, Y. Li, X. Li, S. Hu, X. Zhang, W. Xu, S. Thevuthasan, D. R. Baer, J.-G. Zhang, J. Liu, *ACS Nano* **2012**, *6*, 8439; d) M. T. McDowell, S. W. Lee, C. Wang, W. D. Nix, Y. Cui, *Adv. Mater.* **2012**, *24*, 6034; e) F. Wang, H.-C. Yu, M.-H. Chen, L. Wu, N. Pereira, K. Thornton, A. Van der Ven, Y. Zhu, G. G. Amatucci, J. Graetz, *Nat. Commun.* **2012**, *3*, 1201; f) K. He, H. L. Xin, K. Zhao, X. Yu, D. Nordlund, T.-C. Weng, J. Li, Y. Jiang, C. A. Cadigan, R. M. Richards, *Nano Lett.* **2015**, *15*, 1437; g) H. Ghassemi, M. Au, N. Chen, P. A. Heiden, R. S. Yassar, *ACS Nano* **2011**, *5*, 7805.

[12] B. Hertzberg, A. Alexeev, G. Yushin, *J. Am. Chem. Soc.* **2010**, *132*, 8548.

[13] a) G. Zheng, Y. Yang, J. J. Cha, S. S. Hong, Y. Cui, *Nano Lett.* **2011**, *11*, 4462; b) M. P. Rossi, H. Ye, Y. Gogotsi, S. Babu, P. Ndungu, J.-C. Bradley, *Nano Lett.* **2004**, *4*, 989.

[14] a) S. Berber, Y.-K. Kwon, D. Tománek, *Phys. Rev. Lett.* **2000**, *84*, 4613; b) J. Che, T. Cagin, W. A. Goddard III, *Nanotechnology* **2000**, *11*, 65; c) K. Evanoff, J. Khan, A. A. Balandin, A. Magasinski, W. J. Ready, T. F. Fuller, G. Yushin, *Adv. Mater.* **2012**, *24*, 533.

[15] Y. Liu, N. S. Hudak, D. L. Huber, S. J. Limmer, J. P. Sullivan, J. Y. Huang, *Nano Lett.* **2011**, *11*, 4188.

[16] F. Wu, H. Kim, A. Magasinski, J. T. Lee, H.-T. Lin, G. Yushin, *Adv. Energy Mater.* **2014**, *4*, 1400196.

[17] a) X. H. Liu, L. Q. Zhang, L. Zhong, Y. Liu, H. Zheng, J. W. Wang, J.-H. Cho, S. A. Dayeh, S. T. Picraux, J. P. Sullivan, *Nano Lett.* **2011**, *11*, 2251; b) Y. Yuan, A. Nie, G. M. Odegard, R. Xu, D. Zhou, S. Santhanagopalan, K. He, H. Asayesh-Ardakani, D. D. Meng, R. F. Klie, *Nano Lett.* **2015**, *15*, 2998.

[18] K. Zhang, L. Wang, Z. Hu, F. Cheng, J. Chen, *Sci. Rep.* **2014**, *4*, 6467.

[19] Z. Lin, Z. Liu, N. J. Dudney, C. Liang, *ACS Nano* **2013**, *7*, 2829.

[20] a) F. Mizuno, A. Hayashi, K. Tadanaga, M. Tatsumisago, *Adv. Mater.* **2005**, *17*, 918; b) R. Komiya, A. Hayashi, H. Morimoto, M. Tatsumisago, T. Minami, *Solid State Ionics* **2001**, *140*, 83; c) K. Takada, *Acta Mater.* **2013**, *61*, 759; d) K. Takada, *Langmuir* **2013**, *29*, 7538; e) M. Agostini, Y. Aihara, T. Yamada, B. Scrosati, J. Hassoun, *Solid State Ionics* **2013**, *244*, 48.

[21] a) S. Xin, L. Gu, N.-H. Zhao, Y.-X. Yin, L.-J. Zhou, Y.-G. Guo, L.-J. Wan, *J. Am. Chem. Soc.* **2012**, *134*, 18510; b) F. Wu, J. T. Lee, N. Nitta, H. Kim, O. Borodin, G. Yushin, *Adv. Mater.* **2015**, *27*, 101; c) H. Kim, F. Wu, J. T. Lee, N. Nitta, H. T. Lin, M. Oschatz, W. I. Cho, S. Kaskel, O. Borodin, G. Yushin, *Adv. Energy Mater.* **2015**, *5*, 1401792.

[22] a) J. R. Akridge, Y. V. Mikhaylik, N. White, *Solid State Ionics* **2004**, *175*, 243; b) P. G. Bruce, S. A. Freunberger, L. J. Hardwick, J.-M. Tarascon, *Nat. Mater.* **2012**, *11*, 19.

